J|A|C|S
ARTICLES
Published on Web 02/12/2005

Hydrogen Elimination from a Hydroxycyclopentadienyl Ruthenium(II) Hydride: Study of Hydrogen Activation in a Ligand−Metal Bifunctional Hydrogenation Catalyst

Charles P. Casey,* Jeffrey B. Johnson, Steven W. Singer, and Qiang Cui*

Contribution from the Department of Chemistry, University of Wisconsin−Madison, Madison, Wisconsin 53706

Received October 28, 2004; E-mail: casey@chem.wisc.edu

Abstract: At high temperatures in toluene, [2,5-Ph_2-3,4-Tol_2(η^5-C_4COH)]Ru(CO)$_2$H (**3**) undergoes hydrogen elimination in the presence of PPh_3 to produce the ruthenium phosphine complex [2,5-Ph_2-3,4-Tol_2-(η^4-C_4CO)]Ru(PPh_3)(CO)$_2$ (**6**). In the absence of alcohols, the lack of RuH/OD exchange, a rate law first order in Ru and zero order in phosphine, and kinetic deuterium isotope effects all point to a mechanism involving irreversible formation of a transient dihydrogen ruthenium complex **B**, loss of H_2 to give unsaturated ruthenium complex **A**, and trapping by PPh_3 to give **6**. DFT calculations showed that a mechanism involving direct transfer of a hydrogen from the CpOH group to form **B** had too high a barrier to be considered. DFT calculations also indicated that an alcohol or the CpOH group of **3** could provide a low energy pathway for formation of **B**. PGSE NMR measurements established that **3** is a hydrogen-bonded dimer in toluene, and the first-order kinetics indicate that two molecules of **3** are also involved in the transition state for hydrogen transfer to form **B**, which is the rate-limiting step. In the presence of ethanol, hydrogen loss from **3** is accelerated and RuD/OH exchange occurs 250 times faster than in its absence. Calculations indicate that the transition state for dihydrogen complex formation involves an ethanol bridge between the acidic CpOH and hydridic RuH of **3**; the alcohol facilitates proton transfer and accelerates the reversible formation of dihydrogen complex **B**. In the presence of EtOH, the rate-limiting step shifts to the loss of hydrogen from **B**.

Introduction

The development of new ligand−metal bifunctional hydrogenation catalysts is dramatically changing the face of reduction chemistry.[1] These catalysts provide attractive "green" alternatives to stoichiometric $LiAlH_4$ and $NaBH_4$ reductions and utilize environmentally friendly terminal reductants, such as hydrogen and 2-propanol.[2] The active reducing agent in each of these catalytic systems contains electronically coupled acidic and hydridic hydrogens, which work in concert to efficiently hydrogenate polar unsaturated substrates. The first ligand−metal bifunctional catalyst, the hydroxycyclopentadienyl diruthenium bridging hydride (**1**), was reported by Shvo in the mid 1980s.[3] Since then, Noyori has led the development of these catalysts, including the ruthenium(diamine)(BINAP) catalyst (**2**), which has displayed extraordinary activity in the asymmetric reduction of ketones (Figure 1).[1,4]

Our group has reported studies on both the tolyl-substituted analogue of Shvo's hydroxycyclopentadienyl ruthenium hydride (**3**) and Noyori's arene-Ru(II)-TsDPEN [(*N*-*p*-toluenesulfonyl)-1,2-diphenylethylenediamine] hydride (**4**).[5] On the basis of detailed mechanistic studies, including the observation of primary deuterium isotope effects on both hydridic and acidic hydrogens, our group has provided experimental evidence supporting a concerted hydrogen transfer mechanism from the active reducing species **4** to carbonyls and of **3** to carbonyls and imines (Figure 2).[6,7] Noyori has performed theoretical calculations that support this concerted hydrogen transfer from species **4**.[8]

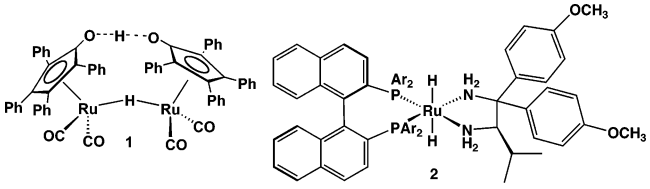

Figure 1. Examples of ligand−metal bifunctional catalysts.

Although the mechanism for reduction in these systems is well understood, evidence for the mechanism of heterolytic

(1) Noyori, R.; Ohkuma, T. *Angew. Chem., Int. Ed.* **2001**, *40*, 40.
(2) Fehring, V.; Selke, R. *Angew. Chem., Int. Ed.* **1998**, *37*, 1827.
(3) (a) Shvo, Y.; Czarkie, D.; Rahamim, Y.; Chodash, D. F. *J. Am. Chem. Soc.* **1986**, *108*, 7400. (b) Menashe, N.; Shvo, Y. *Organometallics* **1991**, *10*, 3885. (c) Menashe, N.; Salant, E.; Shvo, Y. *J. Organomet. Chem.* **1996**, *514*, 97.
(4) The active species has been identified as the trans-dihydride structure: (a) Abdur-Rashid, K.; Faatz, M.; Lough, A. J.; Morris, R. H. *J. Am. Chem. Soc.* **2001**, *123*, 7473. (b) Abdur-Rashid, K.; Clapham, S. E.; Hadzovic, A.; Harvey, J. N.; Lough, A. J.; Morris, R. H. *J. Am. Chem. Soc.* **2002**, *124*, 15104.
(5) (a) Haack, K.-J.; Hashiguchi, S.; Fujii, A.; Ikariya, T.; Noyori, R. *Angew. Chem., Int. Ed. Engl.* **1997**, *36*, 285. (b) Noyori, R.; Hashiguchi, S. *Acc. Chem. Res.* **1997**, *30*, 97. (c) Matsumura, K.; Hashiguchi, S.; Ikariya, T.; Noyori, R. *J. Am. Chem. Soc.* **1997**, *119*, 8738.
(6) Casey, C. P.; Johnson, J. B. *J. Org. Chem.* **2003**, *68*, 1998.
(7) Casey, C. P.; Singer, S. W.; Powell, D. R.; Hayashi, R. K.; Kavana, M. *J. Am. Chem. Soc.* **2001**, *123*, 1090.
(8) Yamakawa, M.; Ito, H.; Noyori, R. *J. Am. Chem. Soc.* **2000**, *122*, 1466.

10.1021/ja043460r CCC: $30.25

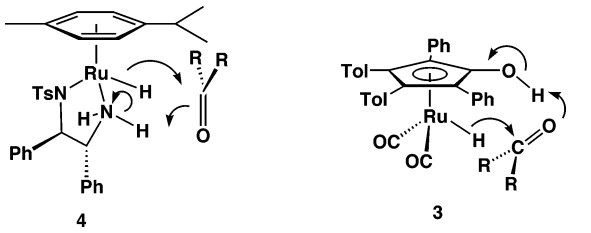

4 **3**

Figure 2. Concerted hydrogen transfer from ligand−metal bifunctional catalysts.

Scheme 1

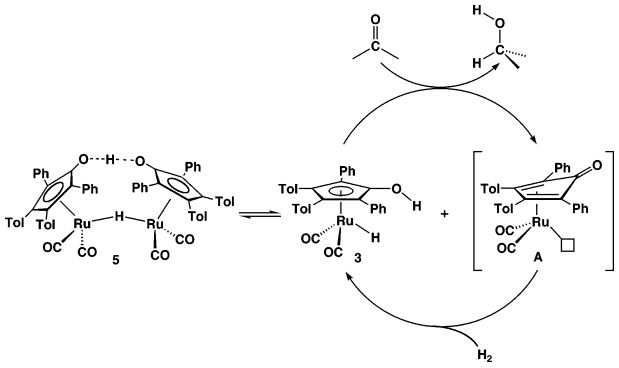

cleavage of hydrogen has remained elusive. In catalytic reduction by the Shvo catalyst, the rate of substrate reduction depends on the rate of hydrogen cleavage. A detailed understanding of this process may assist in the development of more active catalysts.

Noyori's arene-Ru(II)-TsDPEN catalyst **4** is a transfer hydrogenation catalyst which utilizes 2-propanol or a formic acid/triethylamine system as the terminal reductant. The catalytic cycle is completed by regenerating the active reducing species **4** by hydrogen transfer from 2-propanol to the stable 16 electron species via the microscopic reverse of ketone reduction.

Shvo's hydroxycyclopentadienyl ruthenium system is a direct hydrogenation system, using hydrogen to regenerate active species **3**. This regeneration presumably occurs through hydrogen cleavage by intermediate **A**, which is formed upon dissociation of the tolyl-substituted diruthenium bridging hydride **5** or by transfer of hydrogen from **3** to an unsaturated substrate (Scheme 1).

The microscopic reverse of molecular hydrogen cleavage, hydrogen formation, has been proposed to occur at the crystallographically characterized active sites of iron-only hydrogenases isolated from *Desulfovibrio desulfuricans* and *Clostridium pasteurianum*.[9] The active site of Fe-only hydrogenases is a six Fe cluster containing an Fe_4S_4 subsite and an organometallic 2Fe subsite where reversible hydrogen formation may occur by ammonium cation protonation of an intermediate Fe−H (Figure 3).

Although there are several proposed mechanisms for hydrogen cleavage and hydrogen evolution, experimental information is limited and will be addressed in the discussion. To gain further understanding of hydrogen cleavage, as well as additional insight into its overall catalytic cycle, we initiated study of the mechanism of heterolytic hydrogen cleavage by the Shvo catalyst.

(9) Evans, D. J.; Pickett, C. J. *Chem. Soc. Rev.* **2003**, *32*, 268 and references therein.

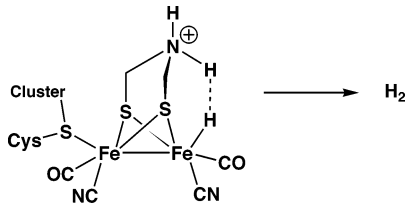

Figure 3. Proposed mechanism of hydrogen formation in iron-only hydrogenases.

Scheme 2

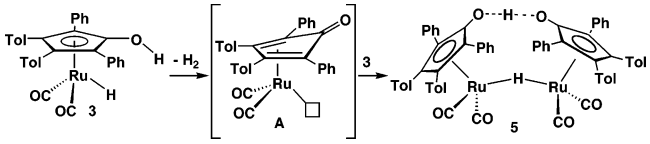

Scheme 3

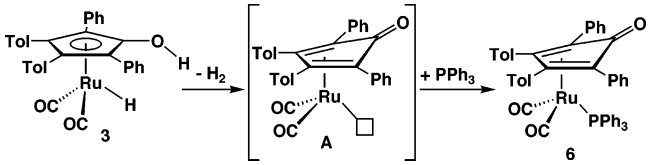

Results

Loss of H_2 from Ruthenium Hydride 3. During catalytic reduction of an unsaturated polar species, a proton and hydride are transferred from ruthenium hydride **3** through a concerted mechanism. In addition to the alcohol product, unsaturated ruthenium species **A** is proposed to result from transfer of hydrogen (Scheme 1). Due to the reactive nature of this proposed intermediate, it has been neither isolated nor spectroscopically observed. As a result, hydrogen cleavage by this species cannot be studied directly. During the course of our previous studies on the Shvo catalytic system, we have observed the slow loss of hydrogen from ruthenium hydride at high temperatures in toluene. We initiated a detailed study on the loss of hydrogen from ruthenium hydride **3** in order to gain greater mechanistic understanding of its microscopic reverse, the hydrogen cleavage process.

Upon loss of hydrogen from ruthenium hydride **3**, we observed the simultaneous formation of diruthenium bridging hydride **5**, which is proposed to occur via the trapping of unsaturated intermediate **A** by a second equivalent of **3** (Scheme 2). Use of ^{1}H NMR spectroscopy in toluene-d_8 allows observation of the disappearance of the hydride resonance of **3** [δ −9.55 (RuH)] and the concurrent appearance of the hydride resonance from dimer **5** [δ −17.82 (RuHRu)]. The resulting hydride disappearance follows first-order kinetics, resulting in a rate of $k_{obs} = 7.13 \times 10^{-4}$ s^{-1} at 95 °C. This rate corresponds to twice the rate of hydrogen loss from ruthenium hydride **3**, as one equivalent loses hydrogen while a second equivalent functions to trap **A**.

Addition of an excess of PPh_3 to the reaction mixture resulted in the formation of triphenylphosphine complex **6**, rather than diruthenium complex **5**, upon loss of hydrogen from **3**. This observation is consistent with the formation of intermediate **A** and subsequent trapping by triphenylphosphine (Scheme 3). These reactions were monitored at 95 °C using ^{1}H NMR spectroscopy to observe the disappearance of ruthenium hydride resonances and the appearance of those consistent with ruthe-

Table 1. Rate of Hydrogen Loss from **3** in the Presence of Different Phosphines in Toluene-d_8

phosphine	T (°C)	k (10^4 s^{-1})
P(m-Tol)$_3$	99	5.95
PPh_3	99	5.57
PMe_3	95	14.23
PPh_3	95	3.52

nium phosphine complex **6** [δ 7.75 (aryl) and 1.90 (tolyl)]. Disappearance of the ruthenium hydride follows first-order kinetics for over three half-lives.

The rate of hydrogen loss was independent of PPh_3 concentration over the range of 0.01−0.06 M, remaining constant at half that of the reaction without phosphine ($k_{obs} = 3.52 \times 10^{-4}$ s^{-1}). This is expected as intermediate **A**, formed upon hydrogen loss from **3**, is trapped by PPh_3 rather than a second equivalent of **3**. These results indicate a zero-order dependence on PPh_3 concentration when present in superstoichiometric quantities. These observations established a first-order rate law for loss of hydrogen from **3** (eq 1).

$$-\frac{d[\mathbf{3}]}{dt} = k[\mathbf{3}][PPh_3]^0 \qquad (1)$$

The temperature dependence of the rate of hydrogen loss in the presence of PPh_3 was monitored between 83 and 110 °C ($k = 1.03 \times 10^{-4}$ s^{-1} at 83 °C; $k = 1.87 \times 10^{-4}$ s^{-1} at 90 °C; $k = 3.54 \times 10^{-4}$ s^{-1} at 95 °C; $k = 6.90 \times 10^{-4}$ s^{-1} at 100 °C; $k = 15.5 \times 10^{-4}$ s^{-1} at 110 °C). An Eyring plot gave the activation parameters: $\Delta H^{\ddagger} = 26.1 \pm 1.4$ kcal mol^{-1} and $\Delta S^{\ddagger} = -3.7 \pm 3.6$ eu.

Hydrogen Loss from 3 in the Presence of Different Phosphines. Other phosphines were also employed to trap the unsaturated intermediate (**A**) formed by hydrogen loss from **3**. For each phosphine, the rate of hydrogen loss was independent of phosphine concentration when present in stoichiometric concentrations. Loss of hydrogen in the presence of P(m-Tol)$_3$ resulted in the formation of tri(m-Tol)phosphine ruthenium complex **7**. The rate constant at 99 °C ($k = 5.95 \times 10^{-4}$ s^{-1}) was similar to that in the presence of PPh_3.

Surprisingly, however, the presence of PMe_3 accelerated hydrogen loss and formation of PMe_3 complex **8**. This rate was about four times faster ($k = 14.23 \times 10^{-4}$ s^{-1} at 95 °C) than that in the presence of PPh_3 (Table 1). Loss of hydrogen from **3** in the presence of a mixture of PMe_3 and PPh_3 gave a statistical mixture of PPh_3 complex **6** and PMe_3 complex **8**. The rate of hydrogen loss from **3** (0.011 M) was measured in the presence of variable PMe_3 concentration and approximately constant total phosphine concentration ($[PPh_3] + [PMe_3] \approx 0.06$ M) (Figure 4). The rate increased nearly linearly with PMe_3 concentration until reaching approximately stoichiometric quantities relative to **3**, at which point the rate plateaued.

At this point, we did not understand how PMe_3 could affect the rate and yet not appear in the rate law. If both PPh_3 and PMe_3 are simply trapping agents, how could different rates be observed? We will return to this point later.

Minimal Interchange of Ruthenium Hydride and Hydroxyl Hydrogen Prior to Loss of Hydrogen. The possible reversible formation of ruthenium dihydride or ruthenium dihydrogen intermediates prior to formation of the unsaturated intermediate **A** was investigated using deuterium labels to probe

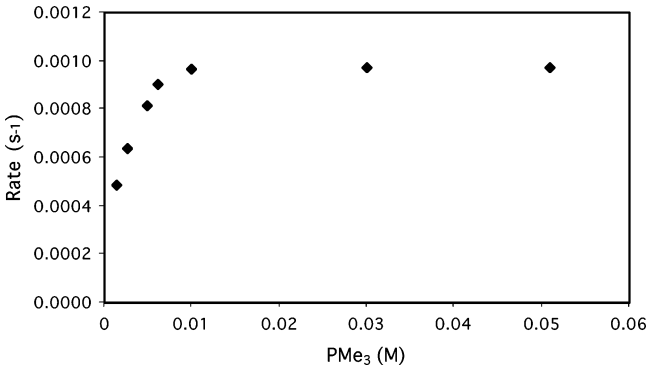

Figure 4. Plot of the rate of hydrogen loss from **3**−**RuHOH** versus concentration of PMe_3 in dry toluene-d_8 at 90 °C, while maintaining constant total phosphine concentration ($[PPh_3] + [PMe_3]$).

Scheme 4

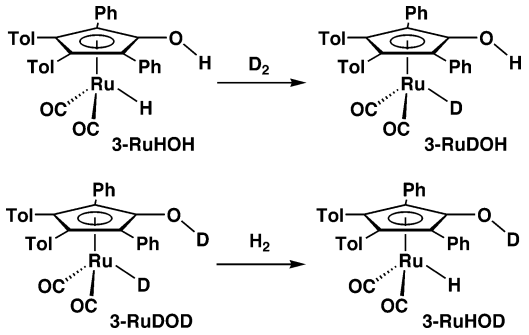

for exchange between the ruthenium hydride and the hydroxyl hydrogen.

Initial preparation of the isotopologs of **3** utilized water to exchange the acidic proton from **3** and **3**−**RuDOD**, which were prepared by literature procedure.[7] The use of water in the exchange led to complications in rate measurements. Despite attempts to remove all water following proton exchange, the presence of residual water led to inconsistent rates of hydrogen loss.

Due to inconsistencies resulting from the presence of residual water, an alternative method was utilized to prepare the isotopologs. Under ~4 atm of D_2 in THF, the ruthenium hydride selectively exchanges with D_2 without exchange of the acidic proton.[10] Using **3**−**RuHOH** and **3**−**RuDOD** as our starting compounds, the final two isotopologs, **3**−**RuDOH** and **3**−**RuHOD**, were prepared by exchange with D_2 and H_2, respectively (Scheme 4).

Hydrogen loss from **3**−**RuDOH** and **3**−**RuHOD** was followed by ^{1}H NMR spectroscopy. Less than 10% of hydrogen exchange between the RuH and CpOH hydrogens was observed. HD (δ 4.47) was the major hydrogen species seen in solution.

Deuterium Isotope Effects On Hydrogen Elimination from Isotopologs of 3. As little or no exchange of deuterium was observed, the rate constant for hydrogen loss from each isotopolog in the presence of PPh_3 was readily determined in toluene-d_8 at 95 °C. These rate constants [**3**−**RuHOH**, $k = (3.52 \pm 0.35) \times 10^{-4}$ s^{-1}; **3**−**RuDOH**, $k = (2.74 \pm 0.14) \times 10^{-4}$ s^{-1}; **3**−**RuHOD**, $k = (2.13 \pm 0.22) \times 10^{-4}$ s^{-1}; and **3**−**RuDOD**, $k = (1.69 \pm 0.12) \times 10^{-4}$ s^{-1}] were compared to determine the kinetic isotope effects (Table 2).

(10) The mechanism of this exchange reaction is not well understood and is currently under investigation.

Scheme 5

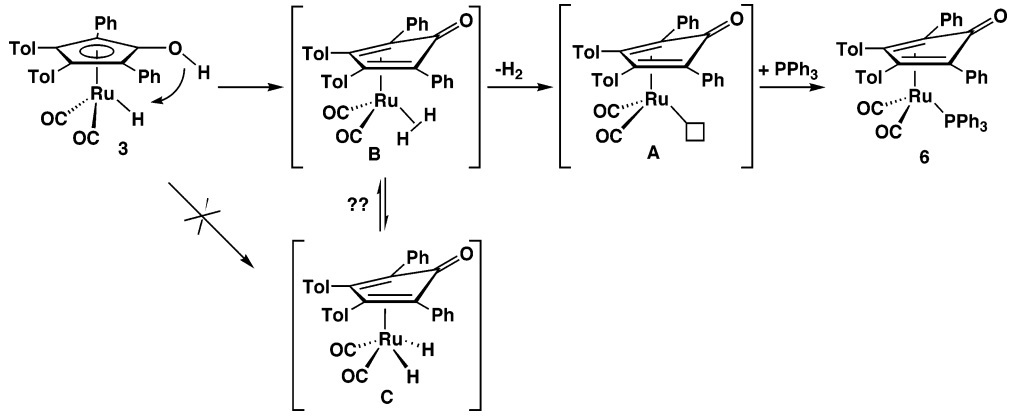

Table 2. Kinetic Isotope Effects for Loss of Hydrogen from Isotopologs of **3** at 95 °C under Alcohol-Free Conditions in Toluene

k_{RuHOH}/k_{RuHOD}	1.65 ± 0.18
k_{RuDOH}/k_{RuDOD}	1.63 ± 0.14
k_{RuHOH}/k_{RuDOH}	1.28 ± 0.14
k_{RuHOD}/k_{RuDOD}	1.26 ± 0.16
k_{RuHOH}/k_{RuDOD}	2.08 ± 0.21

Initial Proposed Mechanism of Hydrogen Elimination from Ruthenium Hydride 3 under Dry Conditions. On the basis of the first-order rate law, we *presumed* that the loss of hydrogen from ruthenium hydride **3** is a unimolecular process (see below for revised mechanism). The activation entropy for this process, $\Delta S^{\ddagger} = -3.7 \pm 3.6$ eu, indicates that the transition state is of similar entropy to the starting materials, consistent with a unimolecular process with neither an associative nor a dissociative process prior to the transition state.

Kinetic isotope effects were observed upon deuteration of either the acidic or the hydridic hydrogen. These isotope effects, $k_{RuHOH}/k_{RuHOD} = 1.65$ and $k_{RuHOH}/k_{RuDOH} = 1.28$, indicate that both the O−H and the Ru−H bonds are broken during either a single step or two steps with similar activation barriers. The product of the individual isotope effects ($1.65 \times 1.28 = 2.11$) lies within error of the observed isotope effect of D_2 loss from the doubly labeled material ($k_{RuHOH}/k_{RuDOD} = 2.08$); this relationship is consistent with a process in which both bonds are broken in a single transition state.

Hydrogen loss from ruthenium hydride **3** is proposed to occur through rate-limiting transfer of the acidic hydrogen. Since no hydrogen exchange between the acidic and hydridic hydrogens was seen, this proton transfer must be irreversible. There are two distinct and distinguishable ways hydrogen transfer might occur: (1) transfer to the ruthenium hydrogen bond could generate ruthenium dihydrogen complex **B**, or (2) transfer to ruthenium could generate ruthenium dihydride **C**.

Kinetic isotope effects allow distinction between these processes. If the rate-determining step had involved transfer of the hydroxyl proton to ruthenium to generate ruthenium dihydride complex **C**, then a significant isotope effect should have been observed only for the hydroxyl group since the ruthenium hydride bond would be largely unchanged. Since we observed a significant isotope effect for the ruthenium hydride ($k_{RuHOH}/k_{RuDOH} = 1.28$), this mechanism can be excluded. In contrast, proton transfer to form ruthenium dihydrogen complex **B** involves a change in both the oxygen−hydrogen and ruthenium−hydrogen bonds, consistent with observed isotope effects on the labeling of each (Scheme 5).

Calculations of Hydrogen Loss from 3. To provide further information about the loss of hydrogen from **3**, a computational study was performed on a simplified model of **3**, in which hydrogens were substituted for the aryl groups on the cyclopentadienyl ring. Computational investigation of the activation energy of uncatalyzed proton transfer from **3** to form **B** predicted a barrier of 43.2 kcal mol^{-1} (including zero-point corrections). Although the imaginary frequency at the transition state (Figure 5) is rather high, 1972*i* cm^{-1}, indicative of a narrow barrier and potentially significant tunneling contribution that are characteristic of hydrogen/hydride transfer reactions, the difference between the computed barrier (43.2 kcal mol^{-1}) and the experimentally determined activation enthalpy (26.1 kcal mol^{-1}) strongly suggests that alternative mechanistic pathways are operative.

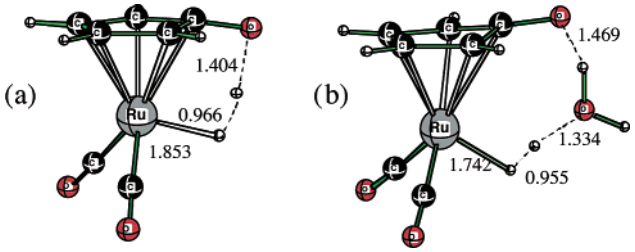

Figure 5. Calculated transition state of (a) uncatalyzed proton transfer and (b) water-facilitated transfer of the acidic proton to the ruthenium hydride of **3**.

Motivated by the Grotthus mechanism proposed for proton translocation in water and biological systems,[11] we explored the possibility of water acting as the proton relay group. Calculations indeed confirmed such a catalytic role of water; the corresponding transition state (Figure 5) was found to be only ~20 kcal mol^{-1} above the hydrogen-bonding complex formed by **3** and a water molecule. Further calculations indicated that a ruthenium dihydrogen complex is a likely intermediate in this process (see Supporting Information for further details).

These results suggest that an agent that can simultaneously donate and accept a proton can effectively catalyze the transfer of the acidic proton to the hydride in order to form a dihydrogen complex, which loses hydrogen to ultimately result in the

(11) von Grotthus, C. J. D. *Ann. Chim.* **1806**, *58*, 54.

Scheme 6

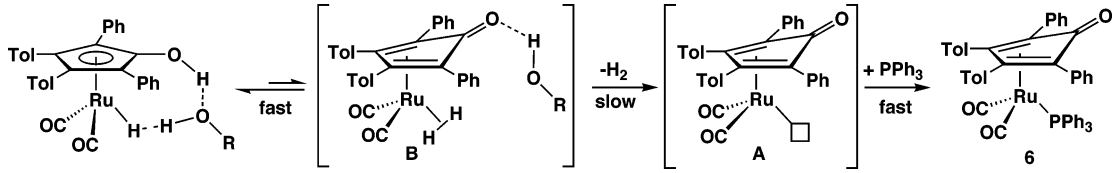

ruthenium phosphine complex. No intermediate dihydride complex was found in the calculations.

These insights prompted us to extend our study to include the observation of hydrogen loss from ruthenium hydride **3** in the presence of water and to re-examine our initial proposal of the hydrogen elimination mechanism under completely dry conditions.

H_2 Loss from 3 is Accelerated by H_2O or Ethanol. Since calculations suggested an intimate role of water in the transfer of hydrogen to form a dihydrogen complex, we systematically studied the effect of water and ethanol on the rate of hydrogen loss from **3**. In the presence of approximately 5 mM water, the rate increased by a factor of 2. Since the dissolution of water in toluene is troublesome, ethanol was used to obtain quantitative kinetic data.

The rate of loss of hydrogen from ruthenium hydride **3** (0.0145−0.0175 M) in the presence of PPh_3 was determined for ethanol concentrations between 0.005 and 0.05 M. The rate increased as ethanol concentration was increased up to approximately 0.03 M, at which point the rate plateaued (Figure 6).

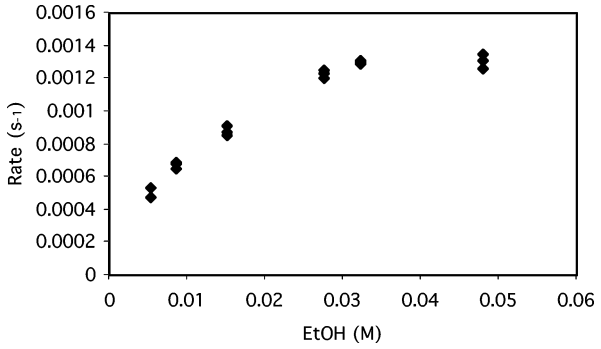

Figure 6. Rate of H_2 loss from **3** versus ethanol concentration in toluene-d_8 at 95 °C.

Fast Ruthenium Deuteride Exchange in the Presence of Ethanol. To determine whether ruthenium deuteride exchanges in the presence of alcohol, the reaction of **3**−**RuDOH** (∼0.01 M) in the presence of excess ethanol (>0.030 M) was monitored by ^{1}H NMR spectroscopy between 56 and 63 °C. The rate of ruthenium deuteride exchange was monitored by the appearance of the ruthenium hydride resonance (δ −9.55). Although the reaction rate was somewhat difficult to measure consistently, the rate was independent of ethanol concentration and displayed first-order dependence upon ruthenium. Approximate rate constants were determined at 56 ($k = 2.03 \times 10^{-3}$ s^{-1}) and 63 °C ($k = 3.66 \times 10^{-3}$ s^{-1}). The activation energy of the exchange was determined from these two values ($\Delta G^{\ddagger} = 23.5$ kcal mol^{-1}) and was used to estimate the rate constant for this reaction at 95 °C. When an activation entropy of $\Delta S^{\ddagger} = 0$ eu is assumed, the rate constant of this process is 86×10^{-3} s^{-1}, approximately 250 times faster than hydrogen loss from **3**−**RuHOH** in the absence of ethanol.[12]

At 95 °C in the presence of ethanol and PPh_3, complete exchange between the hydroxyl proton and ruthenium deuteride of **3**−**RuDOH** was observed prior to significant hydrogen loss. The rate of phosphine complex formation from **3**−**RuDOH** was identical to that from **3**−**RuHOH** in the presence of similar concentrations of alcohol, providing further indication that fast exchange between ruthenium deuteride and the acidic proton had occurred.

Determination of Isotope Effects on Hydrogen Loss in the Presence of Ethanol. Although the fast exchange between ruthenium hydride and the hydroxyl proton in the presence of alcohol prevents the determination of deuterium kinetic isotope effects with mixed isotopologs **3**−**RuHOD** and **3**−**RuDOH**, the isotope effect for the loss of deuterium from **3**−**RuDOD** can be determined in the presence of an excess of deuterated EtOD, again using PPh_3 as the trapping agent. The rate of deuterium loss was measured at two different concentrations of EtOD, and in each case, these rates ($k_{obs} = 4.00 \pm 0.38$ s^{-1} at 0.051 M EtOD and $k_{obs} = 3.92 \pm 0.12$ s^{-1} at 0.032 M EtOD) were significantly slower than those of the corresponding reactions of **3**−**RuHOH** with ethanol. Isotope effects were determined by direct comparison of the rates ($k_{RuHOH}/k_{RuDOD} = 3.3$) and were approximately the same at both 0.032 and 0.051 M EtOD.

Mechanism of Hydrogen Elimination in the Presence of Ethanol. The mechanism of hydrogen elimination from ruthenium hydride **3** in the presence of EtOH must account for the exchange of ruthenium deuteride, faster rate of hydrogen loss, a plateau in rate at high concentrations of EtOH, and larger isotope effects ($k_{RuHOH}/k_{RuDOD} = 3.3$) in the presence of EtOH than in its absence ($k_{RuHOH}/k_{RuDOD} = 2.08$). A mechanism involving fast and reversible formation of ruthenium dihydrogen complex **B** catalyzed by a bridging alcohol molecule, followed by rate-limiting hydrogen loss, is consistent with each of the three phenomena (Scheme 6).[13]

The fast exchange of hydrogen into the ruthenium deuteride occurs via rapid and reversible alcohol-assisted formation of ruthenium dihydride complex **B**. The two hydrogens of the dihydrogen ligand are equivalent; thus either can be transferred back to the oxygen. The result is that the acidic and hydridic hydrogens exchange 250 times more rapidly than the rate in which hydrogen is lost.

In the absence of alcohol, the rate is limited by the formation of dihydrogen complex **B**. The rate of hydrogen loss from **3** is faster in the presence of alcohol because this rate limitation is removed by rapid alcohol-mediated formation of **B**. At ethanol concentrations above 0.03 M, the formation of **B** is rapid and

(12) Assumption of $\Delta S^{\ddagger} = 5.0$ eu extrapolates to a rate constant of 107×10^{-3} s^{-1} at 95 °C, while assumption of $\Delta S^{\ddagger} = -5.0$ eu extrapolates to a rate constant of 69×10^{-3} s^{-1} at 95 °C.

(13) A mechanism involving reversible formation of dihydride intermediate **C** prior to rate-limiting formation of **B** cannot be definitively excluded, although kinetic isotope effect evidence, calculations, and better understanding of the mechanism under dry conditions render this mechanism unlikely.

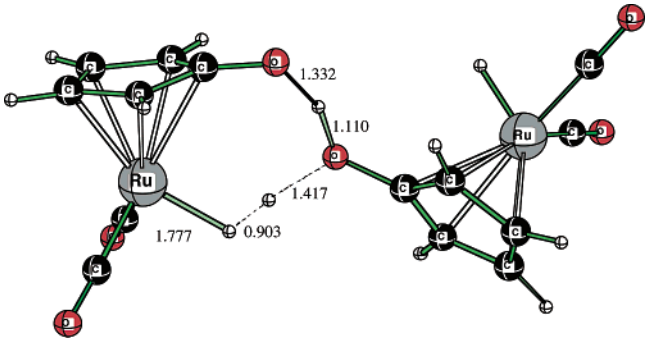

Figure 7. Calculated transition state for formation of dihydrogen intermediate **B** from ruthenium hydride **3** catalyzed by a second equivalent of **3**.

reversible and the rate is determined by hydrogen loss from a very low equilibrium concentration of **B**. The equilibrium between **3** and **B** is responsible for the saturation phenomenon observed at high concentrations of ethanol.

The observed deuterium isotope effect of 3.3 for D_2 loss from **3**−**RuDOD** with EtOD results from a combination of an equilibrium isotope effect on the formation of dihydrogen complex **B** and a kinetic isotope effect on loss of D_2 from **B**. This is different from the 2.08 isotope effect on hydrogen loss from **3**−**RuDOD** in the absence of EtOH, which is a kinetic isotope effect on the formation of dihydrogen complex **B** from **3**.

Problems with Proposed Hydrogen Loss Mechanism in the Absence of Ethanol. Our initial mechanism for hydrogen loss from **3** in the absence of alcohols proposed rate-limiting transfer of the hydroxyl proton to the hydride, forming the H−H bond of dihydrogen complex **B**, followed by rapid loss of dihydrogen (Scheme 5). This proposal was called into question by a calculated barrier for the hydrogen transfer (43.2 kcal mol^{-1}) that was much greater than the experimental value, $\Delta H^{\ddagger} = 26.1$ kcal mol^{-1}. Calculations also suggested that formation of **B** would be greatly facilitated by water or alcohol mediation of transfer of hydrogen from the CpOH group. As outlined above, we have obtained experimental evidence to confirm the predicted role of alcohols. This suggested that in the absence of alcohol, the CpOH unit of a second molecule of **3** might serve as the mediator for the hydrogen transfer leading to dihydrogen complex **B**; calculations on this process predicted an activation barrier of 25.5 kcal mol^{-1} (Figure 7).

While calculations favored the presence of 2 equiv of **3** in the transition state, the kinetic rate law for loss of hydrogen displayed first-order dependence on **3**. The apparent contradiction between two molecules of **3** being involved in the rate-limiting hydrogen transfer and a first-order dependence on **3** could be reconciled if **3** were associated as a hydrogen-bonded dimer in toluene. If the starting material and the transition state both have two ruthenium species, then a kinetic order of one would be observed.

Aggregation State of 3 in Toluene. Pulsed gradient spin−echo (PGSE) NMR measurements were used to determine the state of aggregation of **3** in toluene. The PGSE method provides a means of monitoring the translational motion of a molecule through solution, thereby allowing determination of the diffusion coefficient, *D*, which is inversely related to its hydrodynamic volume.[14] This method has been successfully utilized to assess monomer−dimer equilibria in several organometallic systems.[15]

(14) Price, W. S. *Concepts Magn. Reson.* **1997**, *9*, 299.

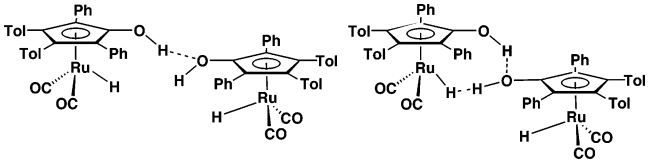

Figure 8. Possible dimerized structure of ruthenium hydride in toluene and transition state for hydrogen transfer to form dihydrogen intermediate **B**.

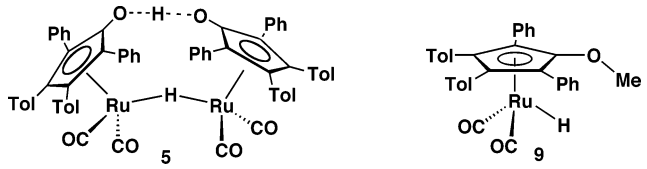

Figure 9. Ruthenium compounds used for PGSE models.

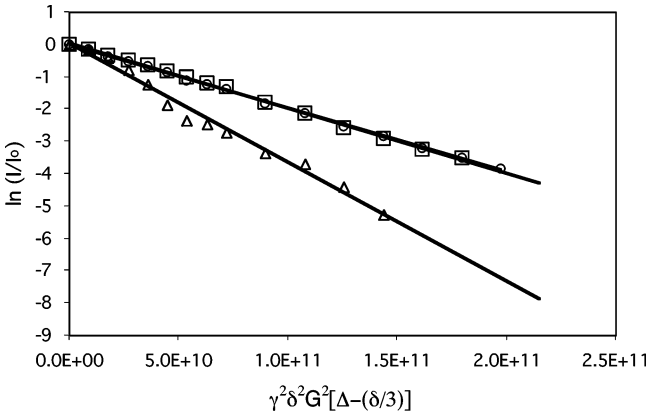

Figure 10. Plot of results of PGSE experiments on **3** (○), **5** (□), and **9** (△). Note that the points and lines for **3** and **5** overlap.

PGSE experiments were performed on toluene-d_8 solutions of **3**−**RuHOH** and on methoxy-protected ruthenium hydride **9** as a model for a monomeric ruthenium compound and on diruthenium bridging hydride complex **5** as a model for a dimer (Figure 9).

The intensity of the Cp tolyl methyl resonances (δ 1.87) of **3**−**RuHOH** in toluene-d_8 (6.6 mg mL^{-1}, 0.0115 M)[16] was measured as a function of diffusion time, which was varied between 25 and 400 ms. Similar measurements were performed on solutions of **5** (δ 1.79) and **9** (δ 1.85). Figure 10 shows plots of $\ln(I/I_o)$ (where I is the intensity in the presence of the gradient, and I_o is the intensity in the absence of a gradient) versus a function of diffusion time with a constant gradient strength. Each point on the plot represents the resonance intensity utilizing a different diffusion time. The slopes of the resulting plots provide the diffusion coefficient, *D*, for each compound, as shown in eq 2. The absolute value of the slope decreases with increasing hydrodynamic volume, thus providing a means of determining the relative volume of each species. The slope for **3**−**RuHOH** ($D = 2.01 \times 10^{-11}$ m^2 s^{-1}) is nearly equal to that of ruthenium dimer **5** ($D = 1.98 \times 10^{-11}$ m^2 s^{-1}) and substantially different from that of the methoxy-protected monomer **9** ($D = 3.65 \times 10^{-11}$ m^2 s^{-1}). These results indicate that species **3** and **5** have

(15) (a) Williams, C. K.; Breyfogle, L. E.; Choi, S. K.; Nam, W.; Young, V. G., Jr.; Hillmyer, M. A.; Tolman, W. B. *J. Am. Chem. Soc.* **2003**, *125*, 11350. (b) Geldbach, T. J.; Pregosin, P. S.; Albinati, A.; Rominger, F. *Organometallics* **2001**, *20*, 1932. (c) Pichota, A.; Pregosin, P. S.; Valentini, M; Wörle, M.; Seebach, D. *Angew. Chem., Int. Ed.* **2000**, *39*, 153.

(16) Concentration values provided assuming a monomeric state for **3**.

Scheme 7

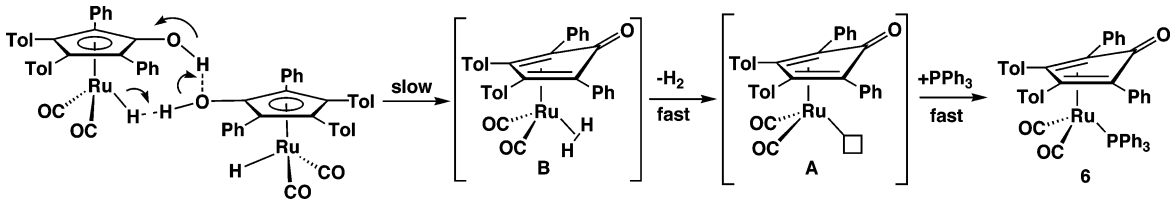

similar hydrodynamic volumes, which is consistent with species **3** existing as a dimer in toluene.[17]

$$\ln \frac{I}{I_o} = \gamma^2 \delta^2 G^2 \left[\Delta - \left(\frac{\delta}{\mathbf{3}}\right)\right] D \qquad (2)$$

where D is the diffusion coefficient, I the intensity of resonance, I_o the intensity of resonance in the absence of gradient, G the gradient strength (4.45 G cm^{-1}), γ the gyromagnetic ratio (4.258×10^3 s^{-1} G^{-1}), δ the length of the gradient pulse (10 ms), and Δ the delay between gradient pulses = diffusion time = varied from 25 to 400 ms.

To determine whether **3** maintains a dimeric structure in the presence of EtOH in toluene-d_8 or whether the dimer is broken up by ethanol solvation, PGSE measurements of **3** (6.3 mg mL^{-1}, 0.0110 M) were carried out in a 0.04 M solution of ethanol in toluene-d_8. The diffusion coefficient ($D = 3.40 \times 10^{-11}$ m^2 s^{-1}) was similar to that obtained for the monomeric model compound **9** ($D = 3.65 \times 10^{-11}$ m^2 s^{-1}). Therefore, ruthenium hydride **3** exists as a monomer in the presence of excess ethanol in toluene-d_8.

A Revised Mechanism of Hydrogen Loss from 3 in the Absence of Ethanol. The PGSE experiments establishing that **3** is a dimer in toluene require a revision of our initial mechanism. The first-order kinetic rate law requires that, as the starting material is dimeric, the transition state must also have two ruthenium species involved. Calculations support the role of the CpOH group of a second molecule of **3** in mediation of proton transfer to form **B** and predict an activation barrier of $\Delta H^{\ddagger} = 25.5$ kcal mol^{-1} for this bimolecular process, very close to the experimental value of $\Delta H^{\ddagger} = 26.1$ kcal mol^{-1} (Figure 7). Since very little exchange between RuH and OD was seen in the absence of ethanol, formation of intermediate **B** must be irreversible and is the rate-limiting step of the overall reaction. Loss of hydrogen from **B** and trapping of the resulting unsaturated intermediate **A** by phosphine occur after the rate-limiting step (Scheme 7).

The RuH kinetic isotope effect ($k_{RuHOH}/k_{RuDOH} = 1.28$) results from the conversion of the ruthenium hydride bond to a dihydrogen complex. The OH kinetic isotope effect ($k_{RuHOH}/k_{RuHOD} = 1.65$) is now seen as involving the two OH bonds that mediate the proton transfer in the formation of dihydrogen complex **B**. All three of these bonds are altered during rate-limiting proton transfer, thus resulting in a doubly labeled isotope effect ($k_{RuHOH}/k_{RuDOD} = 2.08$). This is consistent with the product of the kinetic isotope effects observed upon individual labeling ($1.65 \times 1.28 = 2.11$), indicating that all hydrogen transfers occur in a single step.

Nature of Ruthenium Hydride 3 in Solution with Phosphines. Earlier, we noted that we were puzzled by the faster rates seen in the presence of PMe_3 than in PPh_3 since the phosphines did not appear in the rate law. To further investigate the mechanism of hydrogen loss from **3** in the presence of phosphines, the state of aggregation of **3** in toluene in the presence of added PMe_3 and PPh_3 was investigated by PGSE. In the presence of excess PPh_3 (0.187 M, with 0.0103 M **3**), the intensity of the tolyl methyl group (δ 1.87) was measured as a function of diffusion time, and a plot of $\ln(I/I_o)$ yielded a diffusion coefficient of 1.88×10^{-11} m^2 s^{-1}. This diffusion coefficient is very similar in value to that for ruthenium dimer **5**, consistent with the proposal that complex **3** exists as a dimer in solution in the presence of PPh_3. With an excess of PMe_3 (0.215 M, with 0.0103 M **3**), PGSE gave a diffusion constant of 3.32×10^{-11} m^2 s^{-1}. This diffusion constant is similar in value to that observed for monomeric complex **9**, establishing that in the presence of trimethylphosphine, ruthenium hydride **3** exists as a monomer, presumably hydrogen bonded to PMe_3.

Hydrogen Scrambling in 3−RuDOH in the Presence of PMe_3. When the loss of hydrogen from isotopically labeled **3−RuDOH** in the presence of PMe_3 was monitored by ^{1}H NMR spectroscopy at 95 °C, the observation of a resonance at δ −9.55 indicated that RuD/OH scrambling had occurred. After 10 min, the ratio of RuH:RuD was approximately 1:1, based upon the intensity of the ruthenium hydride resonance relative to that of the tolyl groups of **3** and **6**. This exchange occurred quickly relative to HD loss, and the ratio of RuH:RuD remained near 1:1 throughout the reaction.

Mechanism of Hydrogen Elimination from 3 in the Presence of PMe_3. Although there is no discernible difference in the rate of hydrogen loss from **3** in the presence of PPh_3 and in the complete absence of phosphines, a rate acceleration is observed in the presence of PMe_3. The observation of rate acceleration and saturation in the presence of increasing concentrations of PMe_3, as well as fast exchange between ruthenium hydride and hydroxyl positions, indicates the presence of a mechanism similar to that observed in the presence of alcohol.

PMe_3 is significantly more basic than PPh_3 or P(*m*-Tol)$_3$ and may transfer the acidic hydrogen to the ruthenium hydride via an acid−base reaction to form dihydrogen intermediate **B**. Calculations suggest that PMe_3 can assist in proton transfer and predict a rate-limiting barrier of 25.8 kcal mol^{-1}. Observation of deuterium scrambling and saturation behavior is consistent with the reversible formation of dihydrogen complex **B**, followed by the rate-limiting loss of hydrogen (Scheme 8). Although the means of equilibration between **3** and **B** differ, this mechanism mirrors that of alcohol-catalyzed hydrogen loss.

(17) In principle, ruthenium hydride **3** may also dimerize through metal hydride to acidic proton hydrogen bonding. PGSE studies have indicated that the ruthenium methyl analogue, [2,5-Ph_2-3,4-Tol_2(η^5-C_4COH)]Ru(CO)$_2$CH$_3$, also exists as a dimer in toluene, suggesting that dimerization does not involve the metal hydride unit. The structure involving dimerization through hydrogen bonding of OH groups to one another, shown in Figure 8, is also supported by calculations.

Scheme 8

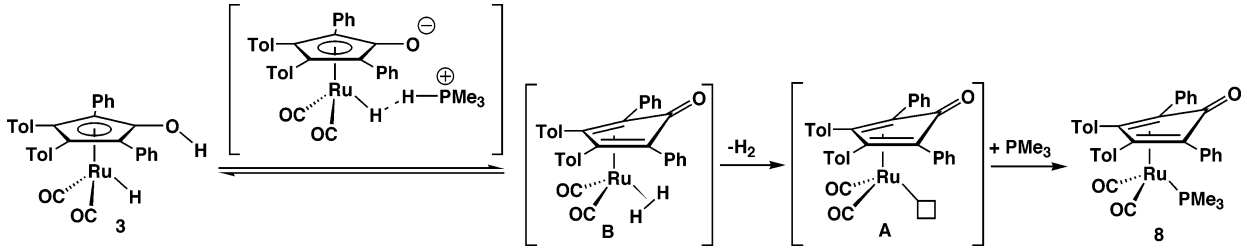

Discussion

Hydrogen Loss from 3 Catalyzed by Ethanol. Determination of the mechanism of hydrogen loss from ruthenium hydride **3** in the presence of ethanol is key to understanding the hydrogenation of carbonyl compounds catalyzed by **3** since alcohols are necessarily present as hydrogenation products. As predicted by our calculations, the presence of alcohol facilitates proton transfer to form dihydrogen complex **B**. This faster rate of proton transfer results in fast RuH/OD exchange, an overall rate increase, and a rate of hydrogen loss independent of ethanol concentration above 0.03 M. PGSE studies have established that in the presence of ethanol in toluene, the hydrogen-bonded dimer of **3** is broken and **3** exists as a monomer, presumably hydrogen bonded to ethanol.

Hydrogen loss from **3** in toluene-d_8 at 95 °C occurs at a similar rate in the presence of high concentrations of ethanol ($k = 13.9 \times 10^{-4}$ s^{-1}) or PMe_3 ($k = 14.2 \times 10^{-4}$ s^{-1}). The similarity of these rate constants is consistent with their related mechanisms. Since both EtOH and PMe_3 catalyze the fast and reversible formation of dihydrogen complex **B**, both rates are expected to be limited in rate by the loss of hydrogen from **B**.

At low concentrations of EtOH or PMe_3, we observed an increase in rate as the concentration was increased (Figures 4 and 6). At these concentrations, ruthenium hydride **3** exists as a mixture of monomer and dimer, there are multiple hydrogen transfer mechanisms, and the kinetics are undoubtedly complex. The rate increase reflects the shift from the slower reaction of dimeric **3** to the faster reaction of monomeric **3** with increasing concentrations of EtOH or PMe_3.

Benefits of Calculations in this Study. Calculations have often provided important support for and insight into organometallic reaction mechanisms. In this case, calculations played a more crucial role in crushing our preconceived mechanism in which the CpOH directly protonates the hydride of **3** to produce dihydrogen complex **B**. Calculations were also important in suggesting the importance of an alternative mechanism involving proton transfer mediated by alcohols in the conversion of **3** to **B**. Computations are particularly valuable when they dispel incorrect mechanistic preconceptions.

Tautomeric Equilibria Involving Metal Hydrides. The equilibrium between ruthenium hydride **3** and dihydrogen intermediate **B** is an example of a tautomeric equilibrium involving a metal hydride. Other examples include (1) metal dihydrogen complexes and their tautomeric metal dihydrides, and (2) complexes in which a metal hydride is intramolecularly hydrogen bonded to an acidic hydrogen and their tautomeric dihydrogen complexes.[18,19]

Alcohol/Alkoxide Promotion of Heterolytic Hydrogen Cleavage during Metal−Ligand Bifunctional Catalysis. The observation of alcohol-promoted elimination from **3** is consistent with a growing body of data that implicate alcohols or alkoxides as promoters of heterolytic H_2 cleavage by homogeneous reduction catalysts operating through a metal−ligand bifunctional mechanism. Ikariya proposed an alcohol-assisted H_2 cleavage for the generation the chiral Cp^*Ru diamine hydride complex **10**, which serves as the active species in catalytic asymmetric hydrogenation of ketones (Scheme 9).[20]

Scheme 9

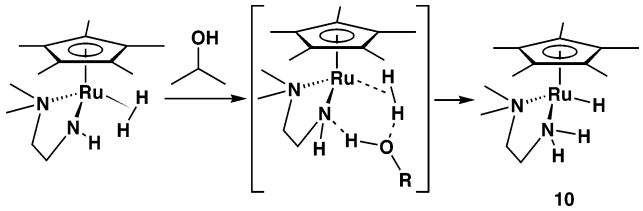

Morris and Rautenstrauch have also reported faster acetophenone hydrogenation by ruthenium dihydride **11** in 2-propanol compared to benzene (Figure 11). Heterolytic hydrogen cleavage

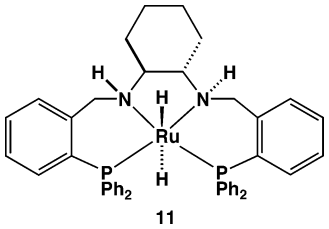

Figure 11. Ruthenium hydrogenation catalyst **11**.

is the rate-limiting step of catalysis, and acceleration is proposed to result from the stabilization of the polar transition state of dihydrogen cleavage by the hydrogen bonding ability and the higher dielectric constant of 2-propanol.[21] The possible role of alcohol as a transfer agent to catalyze the cleavage of hydrogen was not mentioned.

On the basis of theoretical studies of Ru(II)BINAP(diamine) (**1**), Noyori also proposed that the active reducing species is re-formed by cleaving hydrogen either by direct addition across the Ru−N bond or by alcohol-mediated hydrogen transfer via a six-membered transition state (Figure 12).[22] Morris has also contributed to this issue, reporting DFT calculations of proposed intermediates and transition states for the direct cleavage of hydrogen by a model of catalyst **1**.[4b]

(18) Lee, J. C., Jr.; Peris, E.; Rheingold, A. L.; Crabtree, R. H. *J. Am. Chem. Soc.* **1994**, *116*, 11014.
(19) Lough, A. J.; Park, S.; Ramachandran, R.; Morris, R. H. *J. Am. Chem. Soc.* **1994**, *116*, 8356.
(20) Ito, M.; Hirakawa, M.; Murata, K.; Ikariya, T. *Organometallics* **2001**, *20*, 379.
(21) Rautenstrauch, V.; Hoang-Cong, X.; Churlaud, R.; Abdur-Rashid, K.; Morris, R. H. *Chem.—Eur. J.* **2003**, *9*, 4954.
(22) Sandoval, C. A.; Ohkuma, T.; Muñiz, K.; Noyori, R. *J. Am. Chem. Soc.* **2003**, *125*, 13490.

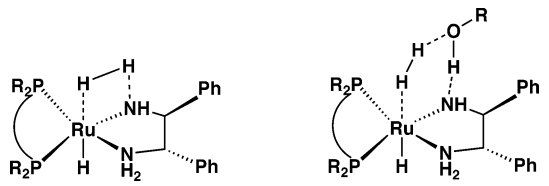

Figure 12. Possible hydrogen cleavage mechanisms for catalyst **1**.

Scheme 10

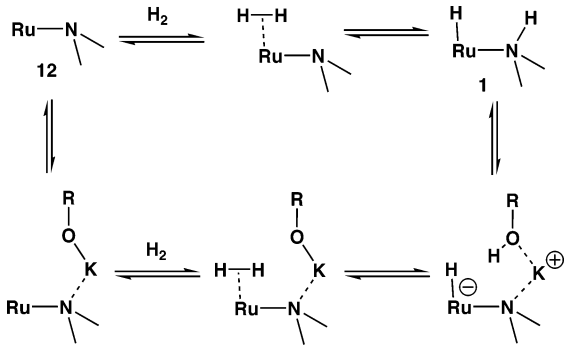

Chen demonstrated that an alkali metal cation is required to achieve high activity in catalytic asymmetric ketone reductions using Noyori's RuH_2(diphosphine)(diamine) system. Chen suggested two possible mechanisms for H_2 cleavage by the unsaturated precursor **12** to form the active reducing species **1** (Scheme 10),[23] one involving direct amido deprotonation of a dihydrogen ligand and the other involving deprotonation of a dihydrogen complex by an alkoxide bound through an alkali metal cation to the amide group on ruthenium. Recently, Noyori has proposed alcohol-assisted H_2 cleavage for catalytic asymmetric ketone reductions under neutral conditions with RuH(η^1-BH_4)[(*S*)-tolbinap][(*S*,*S*)-dpen] as the precatalyst.[22]

Conclusion

Our studies of hydrogen loss from ruthenium hydride **3** have provided significant insight into its mechanistic reverse process, the heterolytic cleavage of hydrogen in the presence of ethanol. Reaction begins with addition of hydrogen to ruthenium unsaturated intermediate **A**, forming dihydrogen complex **B**. Alcohol mediates proton transfer to the carbonyl from **B** to form the active reducing species **3**. This work contributes to a growing body of data underscoring the importance of alcohols in promoting heterolytic hydrogen cleavage in metal bifunctional catalysis.

Experimental Section

General. All syntheses and sample preparations were performed following Schlenk techniques or in a nitrogen atmosphere glovebox. Toluene-d_8 and THF were dried over sodium and benzophenone and distilled prior to use. Solvents were dried with activated alumina purification columns.[24] NMR spectra were recorded on a 360 MHz spectrometer. ^{1}H NMR spectra are referenced to residual protons in deuterated solvent; ^{13}C NMR spectra are referenced to carbon-13 in the deuterated solvent, and ^{31}P NMR are referenced to an external standard of H_3PO_4.

Ruthenium complexes **5**, **3**, and **3**−**RuDOD** were prepared according to literature procedure.[7] Independent synthesis and characterization of **6**, **7**, **8**, and **9** are provided in the Supporting Information.

3−**RuDOH.** Ruthenium species **3** was dissolved in toluene in a resealable NMR tube and degassed with three freeze−pump−thaw cycles. The NMR tube was cooled to −196 °C in liquid nitrogen, and 1 atm of D_2 was added. This mixture was shaken over a period of 2 h at ambient temperature for complete conversion to **3**−**RuDOH**.[10]

3−**RuHOD.** Ruthenium species **3**−**RuDOD** was dissolved in toluene in a resealable NMR tube and degassed with three freeze−pump−thaw cycles. The NMR tube was cooled to −196 °C in liquid nitrogen, and 1 atm of H_2 was added. This mixture was shaken over a period of 2 h at ambient temperature for complete conversion to **3**−**RuHOD**.

General Kinetic Procedure. The general kinetic procedure will be illustrated with a specific example. A standard THF solution of ruthenium species **3** containing ferrocene as an internal standard (0.25 mL, 0.0121 M, prepared in a nitrogen atmosphere glovebox from 8.3 mg of **5**, ∼2 mg of ferrocene, and 0.9 mL of THF) in a resealable NMR tube was degassed with three freeze−pump−thaw cycles. This sample was cooled to −196 °C in liquid nitrogen, and 1 atm H_2 was added. The sample was heated at 85 °C for 8 h to ensure complete formation of ruthenium hydride **3**. The solvent was removed under low pressure. The NMR tube was refilled with N_2, and the solids were dissolved in a standard toluene-d_8 solution of triphenylphosphine (0.35 mL, 0.0543 M, prepared in a nitrogen atmosphere glovebox from 17.1 mg of triphenylphosphine and 1.2 mL of toluene-d_8) added from a 500 μL gastight syringe. The NMR tube was resealed and inserted into an NMR spectrometer preheated to 95 °C. After locking and shimming (∼2 min), we began the data acquisition. The disappearance of ruthenium hydride complex **3** and the appearance of the ruthenium phosphine complex **6** were both followed by ^{1}H NMR spectroscopy for over 2.5 half-lives (∼90 min). The concentration of **3** was followed by measuring the integrations from δ 1.79 to 1.84 and from δ −9.5 to −9.6 (tolyl methyl and hydride resonances, respectively) compared to the integration of the ferrocene internal standard. The concentration of product **6** was followed by measuring the integrations between δ 1.87−1.93 and δ 7.70−7.80 (tolyl methyl and aryl resonances, respectively) compared to the integration of the ferrocene internal standard.

Computational Methods. The geometries for all critical species (reactants, intermediates, transition states, and products) were optimized in the gas phase using the hybrid density functional theory, B3LYP.[25] To simplify calculations, the tolyl and phenyl substituents on the cyclopentadiene of **3** were replaced by hydrogens. The effective core potential (ECP) of Hay and Wadt[26] and the corresponding basis set (augmented by an *f* function) were used for Ru; the 6-31++G(d,p) basis[27] was used for all other main group elements. Vibrational frequency calculations were subsequently carried out to verify the character of the optimized structures and to obtain the zero-point vibrational energy corrections to barrier heights. Solvation effect was estimated to be small (so results not included), using the polarizable continuum model (IEF-PCM[28]) on gas-phase-optimized structures; a dielectric constant of 7.58 was used for tetrahydrofuran (THF) as the solvent. All calculations were performed with the Gaussian98 program.[29]

Acknowledgment. Financial support from the Department of Energy, Office of Basic Sciences, is gratefully acknowledged.

(23) (a) Hartmann, R.; Chen, P. *Angew. Chem., Int. Ed.* **2001**, *40*, 3581. (b) Hartmann, R.; Chen, P. *Adv. Synth. Catal.* **2003**, *345*, 1353.
(24) Pangborn, A. B.; Giardello, M. A.; Grubbs, R. H.; Rosen, R. K.; Timmers, F. J. *Organometallics* **1996**, *15*, 1518.
(25) (a) Becke, A. D. *Phys. Rev. A* **1988**, *38*, 3098. (b) Lee, C.; Yang, W.; Parr, R. G. *Phys. Rev. B* **1988**, *37*, 785. (c) Becke, A. D. *J. Chem. Phys.* **1993**, *98*, 5648.
(26) Hay, P. J.; Wadt, W. R. *J. Chem. Phys.* **1985**, *82*, 299.
(27) (a) Ditchfield, R.; Hehre, W. J.; Pople, J. A. *J. Chem. Phys.* **1971**, *54*, 724. (b) Hehre, W. J.; Ditchfield, R.; Pople, J. A. *J. Chem. Phys.* **1972**, *56*, 2257. (c) Hariharan, P. C.; Pople, J. A. *Theor. Chim. Acta* **1973**, *28*, 213.
(28) (a) Miertus, S.; Scrocco, E.; Tomasi, J. *Chem. Phys.* **1981**, *55*, 117. (b) Cammi, R.; Tomasi, J. *J. Comput. Chem.* **1995**, *16*, 1449. (c) Mennucci, B.; Cancès, E.; Tomasi, J. *J. Phys. Chem. B* **1997**, *101*, 10506. (d) Cancès, E.; Mennucci, B.; Tomasi, J. *J. Chem. Phys.* **1997**, *107*, 3032.

J.J. thanks the ACS Organic Division Emmanuil Troyansky Graduate Fellowship for support. S.S. thanks the NIH (5T32 GM 08505) for support under a Chemistry Biology Interface Training Grant. We also thank Dr. Charles Fry for his valuable assistance with PGSE experiments. Grants from NSF (che-962-9688) and NIH (I S1- RR04981-01) for the purchase of NMR spectrometers are acknowledged.

Supporting Information Available: General experimental methods, experimental details, characterization of complexes **7**, **8**, and **9**, further computational details, and summary of kinetic runs. This material is available free of charge via the Internet at http://pubs.acs.org.

JA043460R

(29) Frisch, M. J.; Trucks, G. W.; Schlegel, H. B.; Scuseria, G. E.; Robb, M. A.; Cheeseman, J. R.; Zakrzewski, V. G.; Montgomery, J. A., Jr.; Stratmann, R. E.; Burant, J. C.; Dapprich, S.; Millam, J. M.; Daniels, A. D.; Kudin, K. N.; Strain, M. C.; Farkas, O.; Tomasi, J.; Barone, V.; Cossi, M.; Cammi, R.; Mennucci, B.; Pomelli, C.; Adamo, C.; Clifford, S.; Ochterski, J.; Petersson, G. A.; Ayala, P. Y.; Cui, Q.; Morokuma, K.; Malick, D. K.; Rabuck, A. D.; Raghavachari, K.; Foresman, J. B.; Cioslowski, J.; Ortiz, J. V.; Stefanov, B. B.; Liu, G.; Liashenko, A.; Piskorz, P.; Komaromi, I.; Gomperts, R.; Martin, R. L.; Fox, D. J.; Keith, T.; Al-Laham, M. A.; Peng, C. Y.; Nanayakkara, A.; Gonzalez, C.; Challacombe, M.; Gill, P. M. W.; Johnson, B.; Chen, W.; Wong, M. W.; Andres, J. L.; Gonzalez, C.; Head-Gordon, M.; Replogle, E. S.; Pople, J. A. Gaussian 98, revision A.6; Gaussian, Inc.: Pittsburgh, PA, 1998.